J. Fluid Mech. (2014), *vol.* 741, R1, doi:10.1017/jfm.2013.667

JFM RAPIDS
journals.cambridge.org/rapids

The quasi-static growth of CO_2 bubbles

Oscar R. Enríquez[1,†], Chao Sun[1], Detlef Lohse[1], Andrea Prosperetti[2] and Devaraj van der Meer[1]

[1]Physics of Fluids Group, Faculty of Science and Technology, University of Twente, PO Box 217, 7500 AE Enschede, The Netherlands

[2]Department of Mechanical Engineering, Johns Hopkins University, 3400 N. Charles Street, Baltimore, MD 21218, USA

(Received 7 October 2013; revised 1 December 2013; accepted 12 December 2013)

We study experimentally the growth of an isolated gas bubble in a slightly supersaturated water–CO_2 solution at 6 atm pressure. In contrast to what was found in previous experiments at higher supersaturation, the time evolution of the bubble radius differs noticeably from existing theoretical solutions. We trace the differences back to several combined effects of the concentration boundary layer around the bubble, which we disentangle in this work. In the early phase, the interaction with the surface on which the bubble grows slows down the process. In contrast, in the final phase, before bubble detachment, the growth rate is enhanced by the onset of density-driven convection. We also show that the bubble growth is affected by prior growth and detachment events, though they are up to 15 min apart.

Key words: bubble dynamics, buoyancy-driven instability, convection

1. Introduction

The diffusion-driven growth of bubbles in supersaturated liquids is a common occurrence in nature and technology. From carbonated drinks (Bisperink & Prins 1994; Barker, Jefferson & Judd 2002; Liger-Belair 2005; Sahu, Hazama & Ishihara 2006; Lee, McKechnie & Devereux 2011) to magmatic melts (Sparks 1978) or oil reservoirs (Pooladi-Darvish & Firoozabadi 1999), molten polymers and metals (Amon & Denson 1984), or even the blood of whales or scuba-divers (Crum & Mao 1996; Chappell & Payne 2006), the appearance of gas bubbles might be anything from beneficial to completely detrimental. They may be responsible for a pleasant flavour enhancement but can also lead to volcanic eruptions or cause decompression sickness or even death.

†Email address for correspondence: oscarenriquez@gmail.com

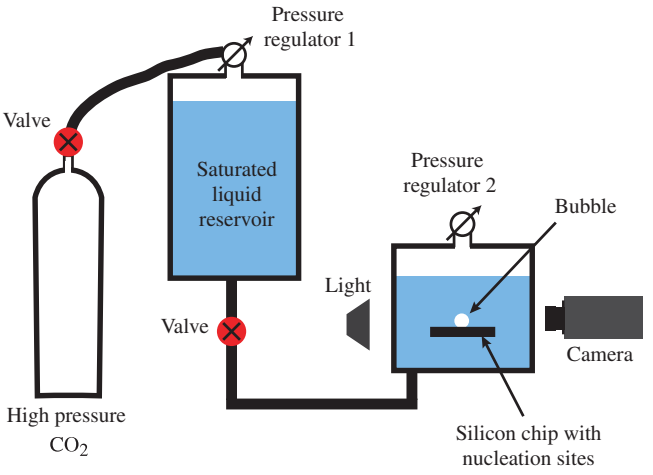

FIGURE 1. Sketch of the experimental system. A saturated aqueous solution of CO_2 is prepared in the reservoir tank and part of it transferred to a smaller observation tank. Here the mix is supersaturated by means of a small, isothermal pressure drop. In order to avoid residual currents in the observation tank, the liquid is allowed to rest for thirty minutes after filling before the pressure is dropped. Temperature is kept stable by circulating water from a refrigerated cooler through a hose wrapped around the tank (see Enríquez *et al.* 2013). A bubble grows from a hydrophobic micro-pit etched on a silicon wafer. The process is imaged through a window in the tank using a long-distance microscope objective with diffuse back light through a window in the opposite side.

Theories, both including (Scriven 1959) and neglecting (Epstein & Plesset 1950) the advective transport induced by the radially expanding bubble interface, predict that the radius R grows proportionally to $\sqrt{t}$ (with a larger prefactor in the former case). Experimental studies using moderately supersaturated water–CO_2 solutions (corresponding to that in a carbonated beverage or beer) have confirmed such time dependence (Bisperink & Prins 1994; Jones, Evans & Galvin 1999; Barker *et al.* 2002).

We perform an experimental study of the controlled growth of a single CO_2 bubble at high pressure ($\sim$6 atm) in a hitherto unexplored low-supersaturation regime, which is an order of magnitude smaller than that of a typical carbonated beverage. In contrast to other works in the moderately supersaturated regime, we find that the concentration boundary layer around the bubble and the substrate on which the latter grows have an important influence on the growth rate.

2. Experimental procedure and results

In the experiment, the desired supersaturation level is induced by a small, isothermal pressure drop in a water–CO_2 solution equilibrated at pressure P_0 and temperature T_0. A suitable and controlled nucleation site is provided by a hydrophobic micro-cavity of radius $R_p = 10$ μm and depth 30 μm, etched in the centre of a small rectangular silicon chip (8 mm × 6 mm). A bubble grows from the pit until buoyancy overcomes the surface tension (estimated as 61 mN m^{-1} in our conditions) that attaches it to the pit, forcing it to detach (Lubetkin & Akhtar 1996). After this, another bubble grows from the same site in a process that can go on for hours. We take images with a digital camera and a long-distance microscope objective at rates of

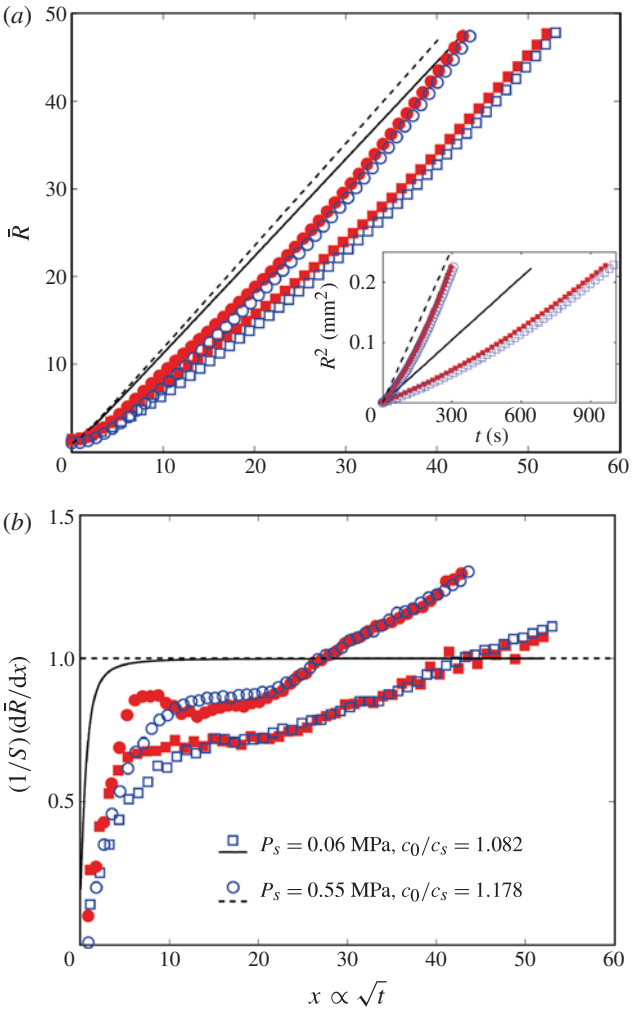

FIGURE 2. Radius (*a*) and its derivative with respect to $\sqrt{t}$ (*b*) in dimensionless form. Symbols represent experimental data. Filled red ones correspond to the first bubble to emerge from the nucleation site and open blue ones to the second. Circles correspond to $c_s = 9.10$ kg m^{-3} and squares to $c_s = 10.01$ kg m^{-3}. In (*a*) the lines represent the full analytical solution of (3.1) for each case. The inset shows the same data and theoretical curves in dimensional form. In (*b*) the theoretical curves for both experimental conditions collapse onto the solid line when they are divided by the asymptotic value S. The local maximum observed for the red circles corresponds to a slight initial overshoot and oscillation of the pressure controller, and therefore is not present in the second bubble. The depressurization is complete and stable at a dimensionless time around 11. For the smaller pressure drop, corresponding to the squares, the overshoot is minimal. The experimental data for this figure are provided as supplementary material available at http//:dx.doi.org/10.1017/jfm.2013.667.

0.5–1 Hz. The smallest bubbles resolvable with our optical resolution (∼2 μm pixel^{-1}) had a radius of about 10 μm. Figure 1 shows a sketch of the experiment and a detailed description of it can be found in Enríquez *et al.* (2013).

Figure 2 shows the results of two different experiments in which the pressure was reduced from the initial value $P_0 = 0.65$ MPa ($T_0 = 21.6$ °C) by 0.05 and 0.1 MPa. Under these conditions it took the bubbles around 5 and 15 min, respectively, to detach. Their final radius, $R_{det} \approx 477$ μm, agrees with the expectation for a quasi-statically grown bubble (Oguz & Prosperetti 1993).

The long detachment times and slow growth rates observed suggest that advection caused by the moving bubble interface is negligible. However, upon comparing experimental results with the corresponding theory, significant discrepancies are evident.

(i) The radius is always smaller than the theoretical prediction and is not proportional to $\sqrt{t}$ (figure 2*a*).

(ii) The derivative $\mathrm{d}R/\mathrm{d}x$, with $x \propto \sqrt{t}$, does not converge to a constant value. Instead, the experimental curves only reach a plateau at a level 20–40 % lower than the theory and they take a longer time to do so (figure 2*b*). Furthermore, the growth rate of the second bubble in each case (open symbols) differs from that of the first one (filled symbols). In figure 2(*b*) it becomes clear that differences are limited to the early growth stages and the two curves for each experiment eventually converge.

(iii) Around $x \sim 20$ there is a point where $\mathrm{d}R/\mathrm{d}x$ starts increasing until eventually it surpasses the maximum predicted by the standard theory summarized below.

In the remainder of this article we disentangle the causes of these differences, which are: (i) the presence of the silicon chip, (ii) a region depleted of CO_2 left behind by the previously detached bubble, and (iii) natural convection triggered by the density difference between liquid in the concentration boundary layer and outside. This last phenomenon stands in contrast to previous experimental studies in which its effects were not detected and therefore explicitly discounted by the authors (Bisperink & Prins 1994; Jones *et al.* 1999).

3. Analysis

3.1. *Idealized problem*

Before getting further in the discussion, let us briefly recall the idealized problem of a bubble growing in an unbounded, supersaturated gas–liquid solution as formulated by Epstein & Plesset (1950). The equilibrium concentration of gas is given by $c_0 = k_H P_0$ (Henry's law), where k_H, Henry's coefficient, is a decreasing function of temperature specific for a given gas–liquid pair. Decreasing the pressure to P_s (at the same temperature T_0) leads to an out-of-equilibrium, supersaturated state. A bubble with an initial radius R_0 is placed in such a supersaturated liquid at $t = 0$. Initially, the concentration is c_0 everywhere, and far from the bubble it is assumed it will remain so. Neglecting the Laplace pressure, the gas concentration at the bubble boundary is constant and given by $c_s = k_H P_s$. For the conditions discussed in this paper, it can be shown that the influence of surface tension is limited to the very first instants of growth, so that it can be neglected throughout. The bubble remains immobile with its centre at the origin of a spherical coordinate system. One can then solve the spherically symmetric diffusion equation to evaluate the time evolution of the concentration gradient at the bubble surface ($r = R$). Equating the gas flow caused by

this gradient to the time derivative of the bubble mass gives an expression for the quasi-static radial growth rate:

$$\frac{\mathrm{d}R}{\mathrm{d}t} = D\beta\left(\frac{1}{R} + \frac{1}{\sqrt{\pi Dt}}\right), \tag{3.1}$$

where $\beta = (c_0 - c_s)/\rho$, $D = 1.97\ \mathrm{m^2\ s^{-1}}$ is the diffusivity of CO_2 in water and $\rho \approx 10\ \mathrm{kg\ m^{-3}}$ is the density of the gaseous phase at P_s. Equation (3.1) can be conveniently expressed in terms of the dimensionless variables $\bar{R} = R/R_p$ and $x = \sqrt{(2D\beta/R_p^2)t}$, where R_p is the radius of the nucleation site. In the original formulation R_0 was used as a length scale; but as this quantity is not defined in the present experiment, we use R_p. Although the full analytical solution to the equation can be obtained (Epstein & Plesset 1950), the asymptotic solution:

$$\bar{R} \approx [\gamma + (1+\gamma^2)^{1/2}]x \equiv Sx \tag{3.2}$$

valid when $\bar{R} \gg 1$ and $x \gg 1$, is a very good approximation. The constant γ is defined as $\gamma = \sqrt{\beta/2\pi}$. The solid line in figure 2(*b*) shows $\mathrm{d}\bar{R}/\mathrm{d}x$ for the complete solution, normalized by its asymptotic value, S, given by the terms inside the brackets in (3.2). We can see here how quickly the full solution to (3.1) converges to this long-term solution (horizontal dashed line in figure 2*b*).

Note that the initial time $t = 0$ of the Epstein–Plesset theory is slightly shifted with respect to the one used in plotting our figures due to the different initial conditions. We could define a virtual initial time by fitting a square-root behaviour to the first few data points, but we do not pursue this possibility as its influence is very small in comparison with the major differences between theory and experiments that are apparent in figure 2.

As the bubble grows, the boundary layer, across which there is a concentration gradient from c_s to c_0, also grows. Its thickness δ (from the bubble surface) grows proportionally to $\sqrt{Dt}$ and soon becomes of the order of, or larger than, the bubble itself (Epstein & Plesset 1950). The assumptions made for the theory imply that $\delta = 0$ at $t = 0$.

We are now in a position to address the issues (i) to (iii) mentioned above.

i. *The role of the silicon chip*

A clear difference between theory and experiments is that in the latter bubbles grow on a substrate instead of in an unbounded medium. This reduces the area available for mass transfer through two effects. First, the bubble is no longer a full sphere, but rather a spherical cap pinned to the perimeter of the nucleation site (Bisperink & Prins 1994; Jones *et al.* 1999; Barker *et al.* 2002). An area equal to the opening of the pit will always be excluded. While such exclusion might be significant for a small bubble, by the time $\bar{R}$ equals 5, it represents only one hundredth of the bubble surface area (see figure 3*a*). Hence, this effect can be considered minimal over the course of the entire bubble lifetime, and clearly it cannot account for the 20–40% reduction observed in the plateau value of $\mathrm{d}\bar{R}/\mathrm{d}x$ (figure 2*b*).

The second effect is that the substrate acts like a barrier which hinders mass transfer into the bubble. This can be qualitatively estimated by removing the mass diffusing across the dashed portion of the bubble surface shown in figure 3(*b*), where the larger sphere denotes the edge of the boundary layer of thickness $\delta = \sqrt{\pi Dt}$. A

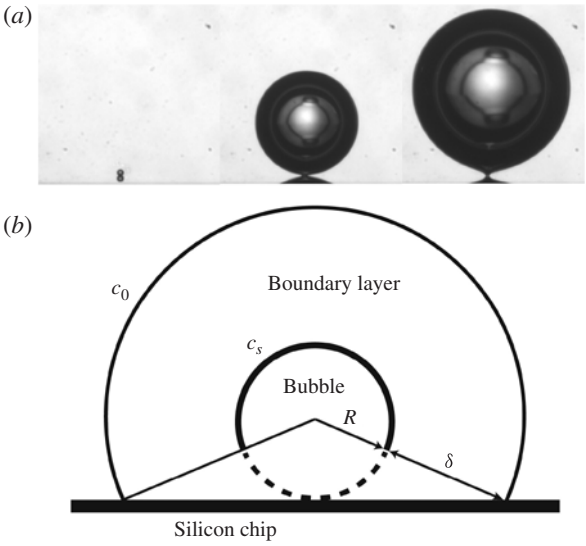

FIGURE 3. (*a*) Images of a growing bubble at $t \approx 1, 152$ and 295 s with $R = 20, 307$ and 474 μm. In the first snapshot, the mirror image of the bubble on the silicon surface is clearly seen below the real bubble. In the other two frames only a small fraction of the reflection is visible. Before dropping the pressure and after each bubble detaches the gas pocket is completely inside the pit and therefore not visible at all. (*b*) Sketch to illustrate the interaction of the concentration boundary layer with the silicon substrate. The excluded bubble area (dashed line) is estimated using the cone formed by the centre of the bubble and the intersection of the boundary layer (shown by the bigger sphere) with the silicon chip.

simple geometrical calculation shows that the remaining 'effective' area of the bubble is given by

$$A_{eff} = 4\pi R^2 \left(1 - \frac{1}{2}\frac{\sqrt{\pi D t}}{R + \sqrt{\pi D t}}\right) \equiv 4\pi R^2 f_A. \tag{3.3}$$

If we repeat the process to derive (3.1) using the diffusion over an area A_{eff} instead of over the full bubble surface area, we recover that same equation multiplied by f_A, the factor inside the parentheses in (3.3). An asymptotic solution can be readily found for the equation, namely

$$\bar{R} \approx \left[\gamma + \left(\frac{1}{2} + \gamma^2\right)^{1/2}\right] x \equiv S^* x, \tag{3.4}$$

where the new term inside the parentheses, S^*, is smaller than S for the unbounded case. In spite of the crude approximations that go into deriving (3.4), the numerical solution to the area-corrected equation (solid and dashed black curves in figure 4*a*) show markedly better agreement with experiments in the range $x = 0$–20.

It is worth noting that another difference with respect to the idealized problem is that by remaining in contact with the silicon chip, the bubble is effectively moving upwards. However it does so at a very small speed, equal to the radial expansion of the bubble ($\dot{R}$). In our experiments, the Péclet number ($Pe = 2R\dot{R}/D$) during the diffusive growth regime (plateau in the curves in figure 2*b*) has values of approximately 0.1 and 0.3, respectively, ruling out the possibility that the bubble translation has a significant effect.

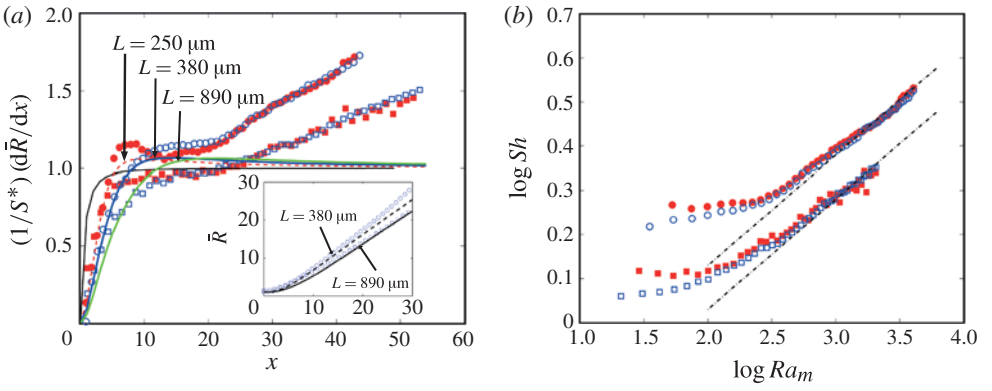

FIGURE 4. (*a*) Experimental $\mathrm{d}\bar{R}/\mathrm{d}x$ rescaled with S^*. Again, circles correspond to $c_s = 9.10$ kg m^{-3} and squares to $c_s = 10.01$ kg m^{-3}, whereas filled symbols correspond to the first and open ones to the second bubble growing in each experimental condition. Lines show corrections for effective diffusion area (solid black curve), and pre-existing boundary layers for the first bubble (red dashed curve) and the second bubble in both experimental conditions (blue, $c_s = 9.9$ kg m^{-3}, and green, $c_s = 9.1$ kg m^{-3} curves). The inset shows the measured time evolution of $\bar{R}$ for the second bubble of both experimental conditions together with its corresponding corrected curve. (*b*) Sherwood number (equation (3.5)) as a function of the mass transfer Rayleigh number. The lines have a slope of 1/4, which indicates that density-driven convection develops around the bubble.

ii. CO_2 *depletion*

Upon detaching, the first bubble leaves behind a region depleted of CO_2, slowing down the growth of the second bubble. This is shown as a delay in reaching the plateau value in the $\mathrm{d}\bar{R}/\mathrm{d}x$ curve (figure 2*b*). Although this phenomenon was considered by Jones *et al.* (1999) and related to the time it takes the following bubble to nucleate, alterations in the growth rate after nucleation were not reported. We introduce the effect of an initially depleted zone into the theoretical model by modifying the initial condition of uniform concentration everywhere to a linear gradient in the radial direction from c_s at $r = R$ to c_0 at $r = L > R$ and uniform concentration farther away. The resulting equation for $\mathrm{d}R/\mathrm{d}t$ is then solved numerically with L as a fitting parameter which is adjusted to match the experimental curves. We found that $L \approx 350$ and 890 μm (figure 4*a*) match the observed slowing down of the respective second bubble growth for the two experimental conditions. Subsequent bubbles, until around the tenth, grow with only minor differences with respect to the second one, which suggests that conditions in the system quickly settle to an approximately steady state. After the tenth bubble (1–3 h into the experiment), the plateau value of the derivative starts to decrease, indicating that the progressive loss of CO_2 in the bulk of the liquid starts to have a noticeable effect on the system.

As shown in figure 4(*a*), fitting of the first bubble growth rate also requires a non-zero value of L, namely $L \approx 250$ μm. A likely explanation is related to the fact that the pressure drop from P_0 to P_s takes place over 30 s. It is conceivable that during this time a concentration gradient of thickness $\sim\sqrt{D \times 30\ \mathrm{s}} \simeq 243$ μm will develop above the pit and hence modify the 'effective' initial conditions for the growing bubble.

iii. *The onset of natural convection*

Finally, we address the transition upward from the plateau value of the $\mathrm{d}\bar{R}/\mathrm{d}x$ curves (figure 2). We conjecture that this increase is due to the onset of buoyancy-driven convection near the bubble caused by the decrease of the density of the solution with decreasing concentration. To support this hypothesis, we recast the experimental data in terms of the Sherwood and Rayleigh numbers:

$$Sh = \frac{2Rh}{D} = \frac{2R\dot{R}}{D\beta} \tag{3.5}$$

$$Ra_m = \frac{g\lambda_c(c_0 - c_s)(2R)^3}{\nu D} \tag{3.6}$$

where $h = \rho\dot{R}/(c_0 - c_s) = \dot{R}/\beta$ is the mass transfer coefficient, g is the acceleration due to gravity, $\lambda_c = 5.9 \times 10^{-4}$ m^3 kg^{-1} is the concentration expansion coefficient of the solution and $\nu = 10^{-6}$ m^2 s^{-1} is the kinematic viscosity. For natural convection around a sphere in an infinite medium it is known that $(Sh - Sh_p) \propto Ra_m^{1/4}$ (Bejan 1993), with the constant $Sh_p = 2$ accounting for pure diffusion. We replot our data in this form (figure 4*b*). The figure shows that initially the Sherwood number is constant, corresponding to diffusive mass transfer. It then starts increasing towards a 1/4 power law, consistent with natural convection around a sphere. This indicates that density-driven convection is developing around the bubble due to the lower density of the fluid in the concentration boundary layer, accelerating the mass transfer rate of CO_2 into the bubble.

4. Conclusions

Why is this phenomenon not observed under a moderate supersaturation ratio? In a carbonated beverage $c_0/c_s = 3$–4, while in our experiments the values were 1.08 and 1.18. At moderate supersaturation, bubbles take well under one minute to reach a 0.5 mm detachment radius and advection by the moving interface is significant (Bisperink & Prins 1994; Jones *et al.* 1999; Barker *et al.* 2002). On the other hand, at our low supersaturations they take 5 to 15 min and advection is negligible. It is plausible that in the first case there is just not enough time for convection to fully develop into a steady state. However it is also conceivable that advection pre-empts density-driven convection by 'squeezing' the boundary layer and keeping it thin. Finally, it is possible too that convection is present in the background, although masked by advection. If so, it might be possible to bring the effect into evidence by consideration of $\mathrm{d}\bar{R}/\mathrm{d}x$, rather than $\bar{R}(x)$, as we have done in figure 2(*b*).

Acknowledgements

We thank H. Lhuissier and L. Stricker for helpful discussions. This work is part of the research programme of the Foundation for Fundamental Research on Matter (FOM), which is part of the Netherlands Organisation for Scientific Research (NWO). We also acknowledge financial support from the National Council for Science and Technology (CONACYT, Mexico), and Shell.

Supplementary figure

Supplementary figure are available at http://dx.doi.org/10.1017/jfm.2013.667.

References

AMON, M. & DENSON, C. D. 1984 A study of the dynamics of foam growth: analysis of the growth of closely spaced spherical bubbles. *Polym. Engng Sci.* **24** (13), 1026–1034.

BARKER, G. S., JEFFERSON, B. & JUDD, S. J. 2002 The control of bubble size in carbonated beverages. *Chem. Engng Sci.* **57** (4), 565–573.

BEJAN, A. 1993 *Heat Transfer*. John Wiley and Sons.

BISPERINK, C. G. J. & PRINS, A. 1994 Bubble growth in carbonated liquids. *Colloids Surf.* A **85**, 237–253.

CHAPPELL, M. A. & PAYNE, S. J. 2006 A physiological model of the release of gas bubbles from crevices under decompression. *Respir. Physiol. Neurobiol.* **153** (2), 166–180.

CRUM, L. A. & MAO, Y. 1996 Acoustically enhanced bubble growth at low frequencies and its implications for human diver and marine mammal safety. *J. Acoust. Soc. Am.* **99** (5), 2898–2907.

ENRÍQUEZ, O. R., HUMMELINK, C., BRUGGERT, G.-W., LOHSE, D., PROSPERETTI, A., VAN DER MEER, D. & SUN, C. 2013 Growing bubbles in a slightly supersaturated solution. *Rev. Sci. Instrum* **84**, 065111.

EPSTEIN, P. S. & PLESSET, M. S. 1950 On the stability of gas bubbles in liquid–gas solutions. *J. Chem. Phys.* **18**, 1505.

JONES, S. F., EVANS, G. M. & GALVIN, K. P. 1999 Bubble nucleation from gas cavities – a review. *Adv. Colloid Interface Sci.* **80** (1), 27–50.

LEE, W. T., MCKECHNIE, J. S. & DEVEREUX, M. G. 2011 Bubble nucleation in stout beers. *Phys. Rev.* E **83**, 051609.

LIGER-BELAIR, G. 2005 The physics and chemistry behind the bubbling properties of champagne and sparkling wines: a state-of-the-art review. *J. Agric. Food Chem.* **53** (8), 2788–2802.

LUBETKIN, S. D. & AKHTAR, M. 1996 The variation of surface tension and contact angle under applied pressure of dissolved gases, and the effects of these changes on the rate of bubble nucleation. *J. Colloid Interface Sci.* **180**, 43–60.

OGUZ, H. N. & PROSPERETTI, A. 1993 Dynamics of bubble growth and detachment from a needle. *J. Fluid Mech.* **257**, 111–145.

POOLADI-DARVISH, M. & FIROOZABADI, A. 1999 Solution-gas drive in heavy oil reservoirs. *J. Can. Petrol. Technol.* **38** (4), 54–61.

SAHU, K. K., HAZAMA, Y. & ISHIHARA, K. N. 2006 Gushing in canned beer: The effect of ultrasonic vibration. *J. Colloid Interface Sci.* **302** (1), 356–362.

SCRIVEN, L. E. 1959 On the dynamics of phase growth. *Chem. Engng Sci.* **10** (1), 1–13.

SPARKS, R. S. J. 1978 The dynamics of bubble formation and growth in magmas: A review and analysis. *J. Volcanol. Geotherm. Res.* **3** (1–2), 1–37.